EPJ Web of Conferences **49**, 14001 (2013)
DOI: 10.1051/epjconf/20134914001

Electroweak Boson Production at LHCb

Kurt Rinnert[1,a], on behalf of the LHCb Collaboration.

[1] *University of Liverpool, Department of Physics*

Abstract. Recent LHCb measurements of W and Z^0 boson production cross-sections, cross-section ratios and jet production in $/\gamma^* Z^0 \to \mu^+\mu^-$ events are reported. Due to the high rapidity coverage and the low momentum trigger thresholds, the LHCb detector can probe previously unexplored regions of the (x, Q^2) space. This allows to further constrain the Parton Density Functions of the proton. Electroweak bosons are reconstructed in several leptonic decay channels, using up to 1 fb^{-1} of pp collisions at $\sqrt{s} = 7$.

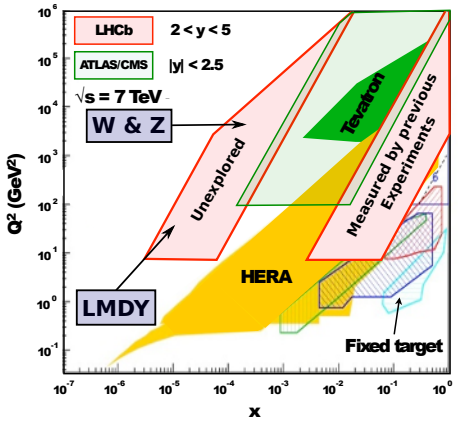

Figure 1: The accessibility of (x, Q^2) space regions by different experiments (from [2]). The region labelled "Unexplored" in the upper left is unique to LHCb. It is accessible by W and Z^0 boson production (higher Q^2) or low mass Drell-Yan (lower Q^2).

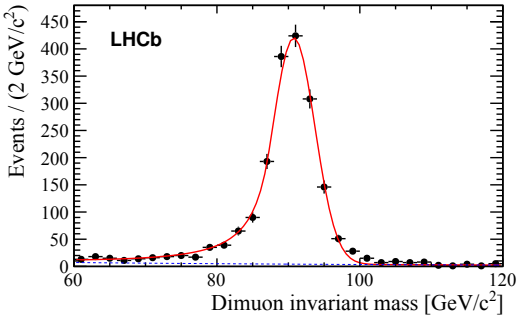

Figure 2: The di-muon invariant mass for the $Z^0 \to \mu^+\mu^-$ event selection.

1 Introduction

The LHCb detector [1] at the CERN Large Hadron Collider (LHC) is a single-arm forward spectrometer covering the pseudorapidity range $2 < \eta < 5$, and has been designed for the study of particles containing b or c quarks. The geometrical coverage for $|\eta| > 2.5$ is unique to LHCb. In this kinematic region, boson production involves a valence quark carrying a large fraction of the proton momentum (high-x) and a sea quark with a small momentum fraction (low-x). This allows to probe Parton Density Functions (PDFs) of the proton in previously unexplored regions of the (x, Q^2) space, as illustrated in Fig. 1.

The relative theoretical uncertainties in NNLO calculations of electroweak boson production are currently at the order of a few percent and are dominated by the PDF uncertainties, which depend on rapidity. Therefore measurements in the unique kinematic range of LHCb can provide valuable inputs to constrain the PDFs [2].

The measurements presented use data from pp collisions at $\sqrt{s} = 7$ recorded by the LHCb experiment in 2010 and 2011. The events are triggered with single lepton triggers with transverse momentum (p_T) thresholds of 10 GeV/c and 15 GeV/c for muons and electrons, respectively.

2 Measurements

2.1 $Z^0 \to \mu^+\mu^-$

The $Z^0 \to \mu^+\mu^-$ events are selected from the full 2010 data set, corresponding to an integrated luminosity of 40 pb^{-1} [3]. The two muons are required to have $p_T > 20$ GeV/c, pseudorapidity in the range $2.0 < \eta < 4.5$ and an invariant mass of $60 < M_{\mu\mu} < 120$ GeV/c^2. The mass requirement ensures consistency with the Z^0 mass. The background sources considered and studied using data and simulation are: $Z^0 \to \tau^+\tau^-$, where both taus decay leptonically to a muon; heavy flavour events with two semi-leptonic decays; generic QCD events where kaons or pions

[a] e-mail: kurt.rinnert@cern.ch

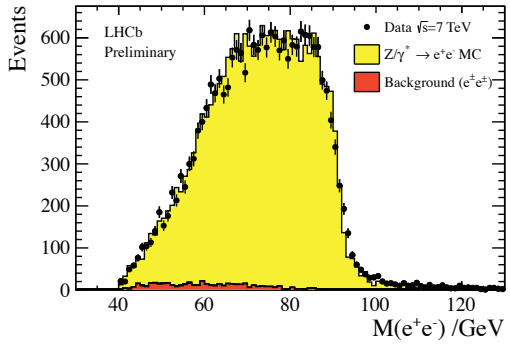

Figure 3: The $Z^0 \to e^+e^-$ momentum spectrum.

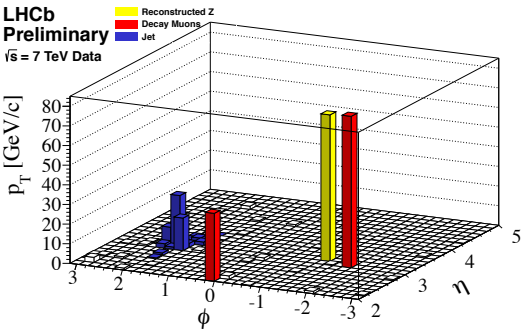

Figure 4: A Z^0 + Jet candidate with $p_{\mathrm{T}}(Z^0) = 27\,\mathrm{GeV}$ and $p_{\mathrm{T}}(\mathrm{Jet}) = 64\,\mathrm{GeV}$.

either decay in flight or punch-through the detector and are falsely identified as muons; top quark and di-boson production. The total number of events passing all criteria is 1966, with a purity of 99.7%. Their invariant mass distribution is depicted in Fig. 2.

2.2 $Z^0 \to e^+e^-$

Data collected in 2011 have been used to select $Z^0 \to e^+e^-$ events [4]. Two identified electrons are required with a p_{T} greater than $20\,\mathrm{GeV}/c$. The pseudo-rapidity is required to be in the interval $2.0 < \eta < 4.5$. A $M_{e^+e^-} > 40\,\mathrm{GeV}/c^2$ cut is applied in order to accommodate for for the saturation of the electromagnetic calorimeter and incomplete Bremsstrahlung recovery. In total, there are 21535 selected candidates with an estimated purity of 98%. The di-electron mass distribution is shown in Fig. 3.

2.3 $Z^0 \to \tau^+\tau^-$

The measurement of the $Z^0 \to \tau^+\tau^-$ cross-section was performed on the $1\,\mathrm{fb}^{-1}$ data set recorded by LHCb in 2011 [5]. Several final states are considered for the tau decays: $\mu^+\mu^-$, μ^+e^-, $e^+\mu^-$, μh or eh, where h refers to an arbitrary hadron. In order to suppress backgrounds like direct leptonic decays, the excellent vertex resolution of LHCb is exploited by requiring significant impact parameters for the tau decay products.

2.4 $\gamma^*Z^0/ \to \mu^+\mu^-$ + Jets

The 2011 data set recorded by LHCb was used to measure the Z^0 + Jets production cross-section [6]. The jet reconstruction uses the FastJet [7] library, using the anti-k_T algorithm with $R = 0.5$. Jets are required to have $p_{\mathrm{T}} > 10$ GeV/c. Figure 4 shows a candidate passing all selection criteria of the Z^0 + jets measurement.

2.5 $W \to \mu\nu_\mu$

The W candidates are selected from the 2010 LHCb data set, corresponding to $40\,\mathrm{pb}^{-1}$ [3]. An isolated muon is required with $p_{\mathrm{T}} > 20$ GeV/c. More stringent selection criteria are required due to the neutrino not being detected in this decay. This is achieved by, *e.g.*, consistency with the primary vertex and exclusion limits imposed on the energy deposited in the hadron calorimeter by muon candidates.

3 Cross-Section Determination

The W and Z^0 cross-section measurements all require leptons in the final state with $p_{\mathrm{T}} > 20$ GeV/c and pseudorapidity in the range $2.0 < \eta < 4.5$. In addition, the Z^0 reconstruction requires consistency with the Z^0 mass, *i.e.* $60 < M_{\mu\mu} < 120$ GeV/c^2. To determine the cross-section, the formula

$$\sigma = \frac{N \cdot \rho}{\mathrm{A} \cdot \epsilon \cdot \int \mathcal{L}} \cdot f_{\mathrm{FSR}}$$

is applied. Here N is the number of selected events, A is an acceptance factor, ρ is the signal purity, ϵ is the overall efficiency and $\int \mathcal{L}$ is the integrated luminosity. The latter is determined by using a Van der Meer scan [8] and a beam gas imaging method [9, 10]. The f_{FSR} factor corrects for the final state radiation. The acceptance A and the f_{FSR} factor are primarily determined from simulation, while efficiencies contributing to ϵ are mostly derived by data-driven methods [3].

4 Results

The $Z^0 \to e^+e^-$ cross section was measured to be $\sigma(Z^0 \to e^+e^-) = 75.7 \pm 0.5(\mathrm{stat}) \pm 2.4(\mathrm{syst}) \pm 2.6(\mathrm{lumi})$ pb [4]. For $Z^0 \to \mu^+\mu^-$ the result is $\sigma(Z^0 \to \mu^+\mu^-) = 76.7 \pm 1.7(\mathrm{stat}) \pm 3.3(\mathrm{syst}) \pm 2.7(\mathrm{lumi})$ pb [3]. A summary of the W and Z^0 cross-sections and ratios for muon final states is presented in Fig. 5. Figure 6 shows the measured $Z^0 \to \tau^+\tau^-$ cross-sections for all considered tau decay final states. Cross-section ratios for Z^0 production vs. the number of associated jets are shown in Fig. 8. The charge asymmetry in W production is shown in Fig. 7.The cross-section uncertainties are summarised in table 1.

All of the results are consistent with theoretical predictions calculated at NNLO using the DYNNLO [11] generator with several different PDF sets.

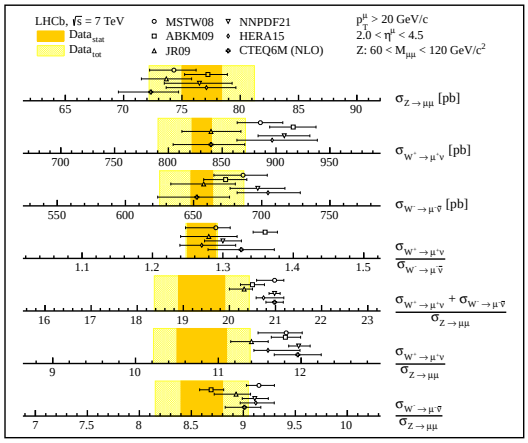

Figure 5: The W and Z^0 cross-sections and ratios for final states with muons. The results (bands) are compared to NNLO predictions with different PDF sets (points).

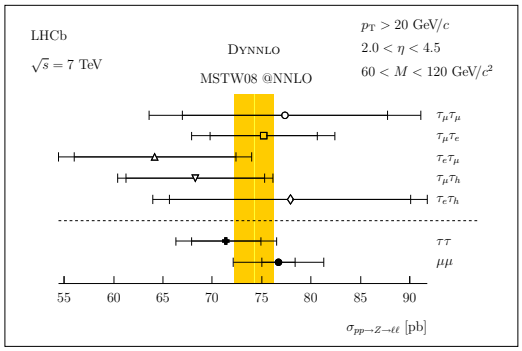

Figure 6: The $Z^0 \to \tau^+\tau^-$ cross-section results for various final states. The results (bands) are compared to NNLO predictions with different PDF sets (points).

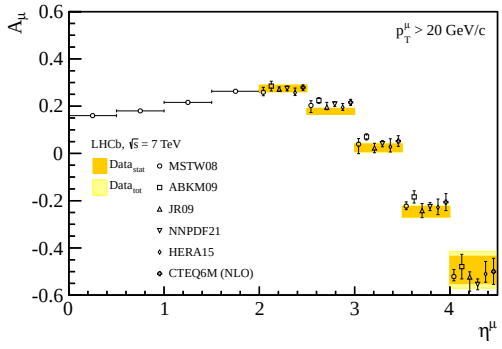

Figure 7: $W \to \mu\nu_\mu$ production charge asymmetry as a function of pseudo-rapidity. The results (bands) are compared to NNLO predictions with different PDF sets (points).

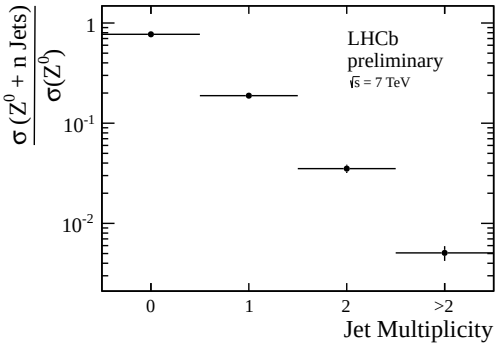

Figure 8: Cross-section ratios vs. the number of associated jets in Z^0 production.

	$\Delta\sigma^Z(\%)$			$\Delta\sigma^W(\%)$	
Source	$\mu^+\mu^-$	e^+e^-	$\tau^+\tau^-$	W^+	W^-
Systematic	**4.3**	3.1	3.9	3.2	2.9
Luminosity	3.5	**3.5**	3.5	**3.5**	**3.5**
Statistical	2.2	0.7	**4.9**	1.1	1.2
Luminosity (pb^{-1})	40	950	1000	40	40

Table 1: Summary of cross-section uncertainties. The dominant uncertainties are highlighted in bold face. The $\tau^+\tau^-$ uncertainties refer to the combination of all final states using BLUE.

References

[1] A.A. Alves Jr. et al. (LHCb collaboration), JINST **3**, S08005 (2008)

[2] R. Thorne, A. Martin, W. Stirling, G. Watt (2008), `arXiv:0808.1847v1 [hep-ph]`

[3] R. Aaij et al. (LHCb collaboration), JHEP **06**, 058 (2012), `1204.1620`

[4] R. Aaij et al. (LHCb collaboration) (2012), `1212.4620`

[5] R. Aaij et al. (LHCb collaboration) (2012), `1210.6289`

[6] *Measurement of jet production in* $Z^0/\gamma^* \to \mu^+\mu^-$ *events at LHCb in* $\sqrt{s} = 7$*TeV pp collisions* (2012)

[7] M. Cacciari, G.P. Salam, Phys.Lett. **B641**, 57 (2006), `hep-ph/0512210`

[8] S. van der Meer, Tech. Rep. CERN-ISR-PO-68-31. ISR-PO-68-31, CERN, Geneva (1968)

[9] M. Ferro-Luzzi, Nucl.Instrum.Meth. **A553**, 388 (2005)

[10] R. Aaij et al. (LHCb collaboration), JINST **7**, P01010 (2012), 1110.2866

[11] S. Catani, M. Grazzini, Phys.Rev.Lett. **98**, 222002 (2007), hep-ph/0703012